A Probabilistic Machine Learning Approach to Detect Industrial Plant Faults

Wei Xiao[1]

[1] *SAS Institute Inc, Cary, NC, 27513, USA*
Wei.Xiao@sas.com

ABSTRACT

Fault detection in industrial plants is a hot research area as more and more sensor data are being collected throughout the industrial process. Automatic data-driven approaches are widely needed and seen as a promising area of investment. This paper proposes an effective machine learning algorithm to predict industrial plant faults based on classification methods such as penalized logistic regression, random forest and gradient boosted tree. A fault's start time and end time are predicted sequentially in two steps by formulating the original prediction problems as classification problems. The algorithms described in this paper won first place in the Prognostics and Health Management Society 2015 Data Challenge.

1. INTRODUCTION

Fault detection in industrial plants is a hot research topic as more and more sensor data are being collected throughout the industrial process, and standard systems based on univariate statistical process control lack power in these more complex systems. Early detection of faults can help to avoid system shut-down and component failure or even catastrophes (Korbicz, Koscielny, Kowalczuk, & Cholewa, 2012).

Many machine learning algorithms used in pattern classification are now being utilized in fault detection. Dimension reduction techniques, such as principal component analysis, partial least squares, and Fisher's discriminant analysis have been applied to detect faults in chemical processes (Chiang, Russell, & Braatz, 2000; Chiang, Kotanchek, & Kordon, 2004; Yin, Ding, Haghani, Hao, & Zhang, 2012). Support vector machine and artificial neural networks are also widely used methods for fault detection; they have been applied to gearbox failure detection (Samanta, 2004) and chemical process fault diagnosis (Wang & Yu, 2005). K-Nearest Neighbor and fuzzy-logic are two other powerful methods that have been used to detect faults in semiconductor manufacturing processes (He & Wang, 2007) and mechanical systems (Korbicz et al., 2012). Tree based algorithms such as random forest and gradient boosted tree are useful machine learning algorithms in situations where one expects nonlinear and interactive effects between covariates. They have been applied to fault detection in aircraft systems (Lee, Park, & Jung, 2014).

This year's Prognostics and Health Management (PHM) Society data challenge focused on plant fault detection. We try many of the above machine learning techniques and ultimately use a combination of several in our final detection strategy described herein. The rest of the paper is organized as follows. Section 2 discusses the data challenge problem. Section 3 introduces the relative methodologies and our algorithm. Finally, Section 4 concludes the paper and discusses future work.

2. PROBLEM STATEMENT

The objective of this year's challenge is to design an algorithm to predict plant faults. Correct prediction involves predicting the type of fault (one of five), as well as the start and end time of each fault, within one hour.

Three datasets are given, training, test, and validation; they contain information on 33, 15, and 15 plants, respectively. For each plant three files are provided: plant-#a.csv, plant-#b.csv, plant-#c.csv, where # is the plant id. File (a) contains time series readings of 4 sensors ($S1$-$S4$) and 4 reference signals ($R1$-$R4$) from each plant component. The number of components (Nm) varies by plant; data on Sj and Rj for ith component are denoted mi_Sj and mi_Rj, respectively, where $i \in \{1, \ldots, Nm\}$ and $j \in \{1, 2, 3, 4\}$. File (b) contains time series data for cumulative energy consumed ($E1$) and instantaneous power ($E2$) from a fixed number of zones within a given plant. Each plant zone covers one or more of the plant components and the number of zones (Nn) varies by plant. The notation ni_Ej is used to represent the reading of Ej for the ith zone. File (c) contains plant fault events, each characterized by a start time, an end time, and a failure type. Data are given on 6 different fault types ($F1 - F6$), but only faults 1-5 are to be predicted. The training dataset has com-

Plant	Nm	Nn	PF1	PF2	PF3	PF4	PF5	PF6
1	6	3	0.25	0.18	0.12	0.04	0.11	0.29
2	13	2	0.46	0.03	0.00	0.02	0.00	0.49
3	10	2	0.17	0.01	0.00	0.02	0.00	0.80
4	8	4	0.30	0.16	0.02	0.02	0.02	0.48
5	3	2	0.27	0.07	0.00	0.07	0.00	0.58
41	5	2	0.29	0.10	0.02	0.05	0.00	0.54
42	10	3	0.39	0.15	0.00	0.07	0.00	0.40
43	6	2	0.08	0.16	0.02	0.22	0.11	0.41
45	7	2	0.17	0.47	0.05	0.06	0.03	0.22
46	5	2	0.19	0.21	0.14	0.05	0.00	0.41

Table 1. Summary statistics of faults by plant. Nm: number of components; Nn: number of zones; $PF1$-$PF6$: proportion of each fault type. (Plants in training set: 1, 2, 3, 4, 5; plants in test set: 41, 42, 43, 45, 46)

plete fault event data, and is used to train the model. The test dataset has complete fault event data for the first half of the sample, but approximately 50% of the events in the second half of the data have been randomly removed. The boundary between the first and second half of the data is given, and referred to as the boundary time. Our goal is to predict the deleted fault events. The validation dataset is similar in structure to the test dataset.

Each team participating in the contest is permitted to submit their predictions of the missing faults in the test data (fault type, and start and end time) once each week to assess their prediction performance and use the score as feedback to improve their model. The final team rank is determined by the score of a submission of predictions based on the validation dataset. The data can be download from NASA Ames Prognostics Data Repository (Rosca, Song, Willard, & Eklund, 2015).

2.1. Data Description and Preprocessing

We began our analysis by first studying the data to garner any information that would be useful in predicting the faults. Not only do the number of both zones and components vary by plant, but the proportion of each fault type (PFi) varies quite dramatically. To illustrate, Table 1 summarizes the data for the first five plants in both the training and test datasets. Note that $F3$ (fault type 3) never occurs in plants 2, 3, 5 and 42, and $F5$ never occurs in plants 2, 3, 5, 41, 42 and 46. We also notice that $S3$, $R1$, $R2$, $R3$, $R4$ appear to be categorical variables, and $S1$, $S2$, $S4$ appear to be continuous variables. The number of unique levels of all categorical variables for the same sample plants are summarized in Table 2. Given the above differences across plants and variables, we built a separate model for each plant.

The sampling interval for the data provided was theoretically 15 minutes, however some logging delays resulted in irregular intervals. To preprocess the data, we rounded all timestamps to obtain regular 15-minute gaps, and then combined

Table 2. Counts of unique levels of all categorical variables. (Plants in training set: 1, 2, 3, 4, 5; plants in test set: 41, 42, 43, 45, 46)

Plant	S3	R1	R2	R3	R4
1	12	38	6	8	3
2	11	26	6	6	3
3	12	30	7	8	3
4	12	34	7	7	3
5	12	12	7	6	3
41	12	33	4	6	3
42	8	38	5	7	3
43	12	23	3	4	3
45	12	23	4	5	3
46	12	40	4	5	3

Timestamp	m1_R1	m1_S1	TTF_F1	start_F1	end_F1
2009-09-04 09:00:00	739	763	-7	0	0
2009-09-04 09:15:00	739	763	-6	0	0
2009-09-04 09:30:00	739	759	-5	0	0
2009-09-04 09:45:00	700	711	-4	1	0
2009-09-04 10:00:00	700	711	-3	1	0
2009-09-04 10:15:00	700	712	-2	1	0
2009-09-04 10:30:00	700	720	-1	1	1
2009-09-04 10:45:00	700	714	0	1	1
2009-09-04 11:00:00	700	716	1	1	1
2009-09-04 11:15:00	700	711	2	1	1
2009-09-04 11:30:00	700	720	-41	1	1
2009-09-04 11:45:00	700	716	-40	1	1
2009-09-04 12:00:00	700	712	-39	0	1
2009-09-04 12:15:00	700	711	-38	0	1
2009-09-04 12:30:00	700	716	-37	0	1
2009-09-04 12:45:00	700	718	-36	0	0

Table 3. A sample of data from plant 1 after preprocessing.

all three files. We define new variables TTF_Fk, $k = 1, \ldots, 6$, to represent time to failure of fault type k. A negative value, $-i$, means the next fault is i intervals in the future (1 interval is 15 minutes), and a positive value, i, means the current fault started i intervals ago and has not yet ended. We define $E3$ as the first order difference of $E1$, i.e., $E3(t) = E1(t) - E1(t-1)$. $E3$ measures the energy consumed in the most recent 15 minutes, which similar as E_2 is a way to measure instantaneous power. We also define $start\_Fk$, $k = 1, \ldots, 6$, as a binary indicator of whether any type k fault starts within one hour of the corresponding timestamp, and define end_Fk, $k = 1, \ldots, 6$, as the binary indicator of whether any type k fault ends within one hour of the corresponding timestamp. Occasionally observations of covariates on some timestamps are missing. Forward imputation was applied to all covariates to impute these missing values, except for TTF_Fk, $start\_Fk$ and end_Fk, which were imputed with values -999, 0 and 0, respectively. To illustrate these preprocessing steps, a small proportion of plant 1's data are shown in Table 3. The imputation simplifies the analysis, and from the authors' observation, it has little influence on the modeling results.

There are segments of time where all covariates are missing and fault type 6 is happening. We assumed the plant must be in some type of maintenance mode during these periods, and

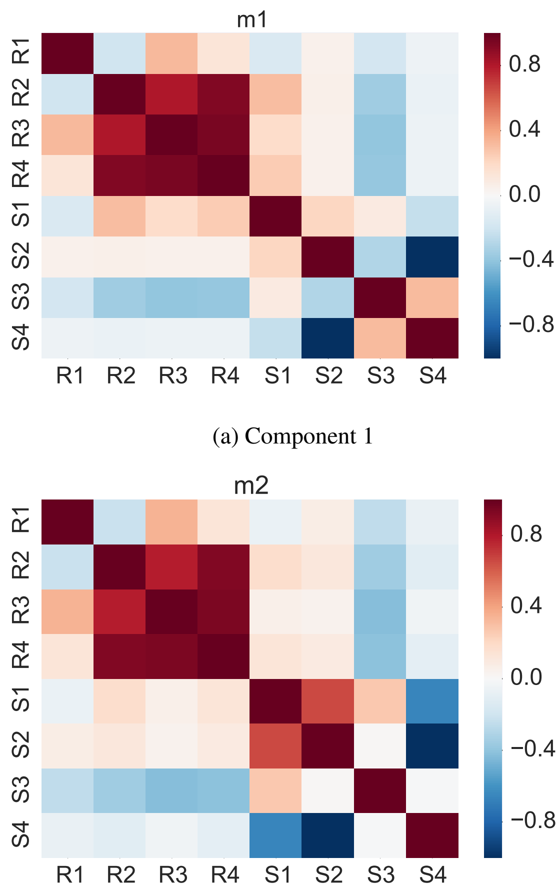

(a) Component 1

(b) Component 2

Figure 1. Correlation heatmap for the first two components of plant 1.

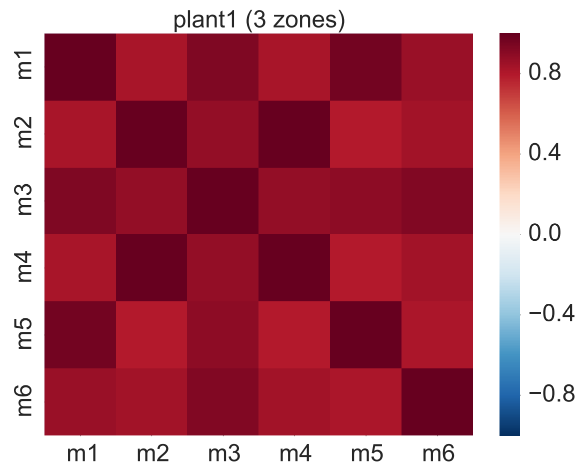

Figure 2. Correlation heatmap of $R4$ across all components in plant 1.

we excluded these observations in the following analysis.

2.2. Visualization

Visualization was key to our understanding of the data.

First, we observe that $R2$, $R3$ and $R4$ are highly positively correlated, and $S2$ and $S4$ are highly negatively correlated, across all components in all plants. To illustrate this finding, Figure 1 shows the correlation heatmap of plant 1 for the first two components, where each cell represents the Pearson correlation between two features. Pearson correlation is calculated as

$$r = \frac{\sum_{i=1}^{n}(x_i - \bar{x})(y_i - \bar{y})}{\sqrt{\sum_{i=1}^{n}(x_i - \bar{x})^2}\sqrt{\sum_{i=1}^{n}(y_i - \bar{y})^2}}.$$

Second, by observing the correlation heatmap of either mi_R2, mi_R3, or mi_R4, across all components for a given plant, one can identify which components are in the same zone; components in the same zone are highly correlated. For example, Figure 2 shows the correlation heatmap of mi_R4 across all 6 components in plant 1. Based on the heatmap, it seems components 1, 3, 5 of plant 1 belong to one zone, components 2, 4 belong to another zone, and component 6 itself belongs to the third zone. Although one can identify which components are zoned together, the groups of components could not always be linked to a specific zone, so this information was ultimately not utilized in our modeling approach.

We also find that month and hour are important categorical variables to predict the faults. Count plots of $F2$ by month and hour are shown in Figure 3 and 4 to illustrate this point. $F2$ starts most frequently between May and November and between 6 o'clock and 23 o'clock. But its distribution varies across plants.

Lastly, we observe that, before a fault happens, sensor readings are often increasing or decreasing. These unique patterns can be utilized to predict the start time of the fault. See Figure 5 for an example, where the mean value of $m2\_R2$ and its corresponding 95% confidence bands are plotted against time to failure of $F1$.

3. METHODOLOGY

In this section we introduce our approach and the related methodologies utilized for the PHM competition. The overall approach consists of two parts: preprocessing and modeling. Figure 6 provides an overview of the process implemented. Details of the data preprocessing have been discussed in Section 2.1. After preprocessing, we divide the training data into two parts: cross validation training data and cross validation test data. Mimicking the test dataset and the validation dataset, the cross validation training data has complete fault

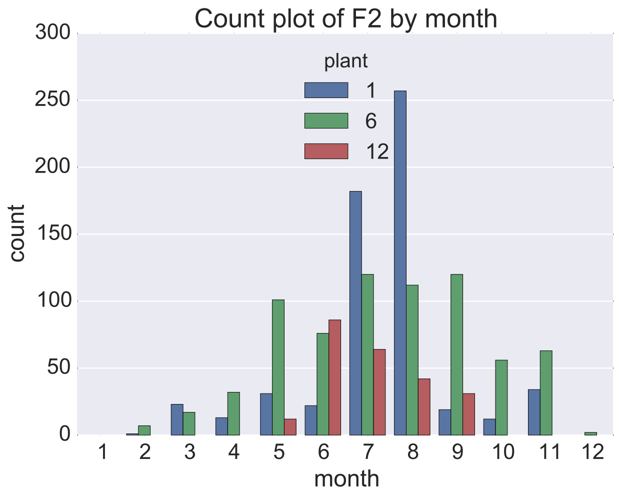

Figure 3. Histogram of fault 2 start times by month (January = 1) for plants 1, 6 and 12.

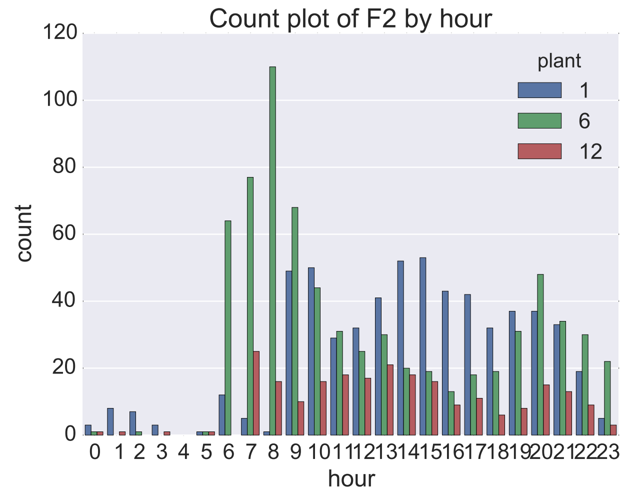

Figure 4. Histogram of fault 2 start times by hour for plants 1, 6 and 12.

event data for the first half of the sample, and 50% randomly selected events in the second half. The cross validation test data contains the 50% deleted events in the second half. Our basic approach is to try various models using the cross validation training data and then evaluate their performance based on their ability to forecast faults in the cross validation test data. The winning model is then applied to the test data and the subsequent predictions submitted to PHM for assessment. Here we are not learning the exact model with cross validation training and test data, as we fit a plant specific model to each plant. However, we learn things such as which classifier to use, which threshold value to apply, etc. Please refer to Section 3.3-3.5 for more details.

There are two steps to the modeling process: predict fault start times and then, given these start times, predict fault end time. A detailed flowchart of the modeling process is shown in Figure 7. The modeling procedure outlined is implemented for each fault type, plant by plant. Given a fault type and plant, $F1$ in plant 5 for example, we translate the prediction problem into a classification problem ($start\_F1$=1 vs $start\_F1$=0). From the classification model we estimate the probability that $F1$ starts during each time interval. We derive the set of predicted fault start times, Ω_{F1}, based on these estimated probabilities. For each start time in Ω_{F1}, we then solve another classification problem (end_F1=1 vs end_F1=0) and estimate the probability the $F1$ will end in the next 1 to $t_{\max}$ time intervals, where $t_{\max}$ is an estimated upper bound of fault $F1$'s duration. These estimated probabilities are used to find the fault end time.

Various machine learning algorithms were tried to solve these classification problems: K-nearest neighbors (KNN), naive bayes, gradient boosting machine (GBM), random forest, penalized logisitic regression (with ℓ_2 penalty), etc. In the final algorithm, we use gradient boosting machine, random forest and penalized logisitic regression. All methods are implemented in SAS or Python Scikit-learn.

In Section 3.1, we give a quick review of the machine learning algorithms used. Section 3.2 discusses how we evaluate the effectiveness of these different approaches. Section 3.3 describes all the features we use in the model and finally, the specific algorithm details to predict a fault's start time and end time are given in Section 3.4 and 3.5, respectively.

3.1. Machine Learning Algorithms

Data-driven or statistical approaches based solely on historical data are seen as the most cost-effective approach for fault detection in complex systems (Aldrich & Auret, 2013). Machine learning is the key to any data-driven algorithm.

Machine learning algorithms can be categorized as either supervised or unsupervised. In supervised learning, the goal is to predict a response Y based on input features X. All methods in our algorithm belong to supervised learning.

K-nearest neighbor is an instance-based learning algorithm which has a very simple form but works extremely well on many problems. The algorithm is simple. For a test point x_0, we first find k training points that are closest in distance to x_0, and then classify using majority vote. K-nearest neighbor can learn very flexible decision boundaries. However, when dealing with high dimensional data, it is likely to suffer from over-fitting and perform poorly due to the curse of dimensionality.

Naive Bayes (Rish, 2001) is a classification technique based on applying Bayes' theorem. It assumes conditional independence between features given a class $Y = i$. Given a class

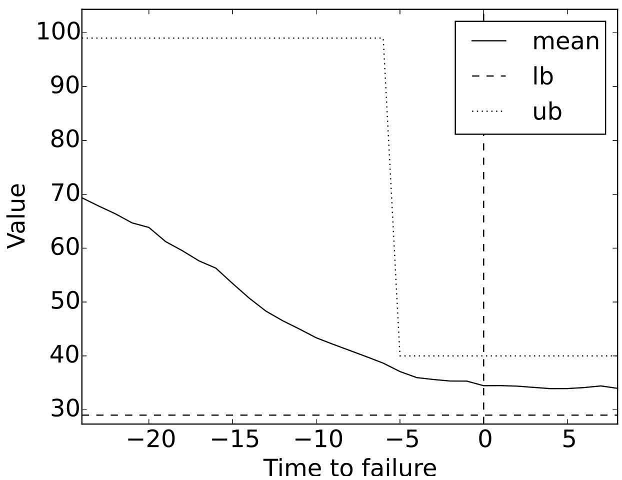

Figure 5. Plot of $m2\_R2$ against time to failure of F1. lb and ub represents 95% lower bound and upper bound respectively.

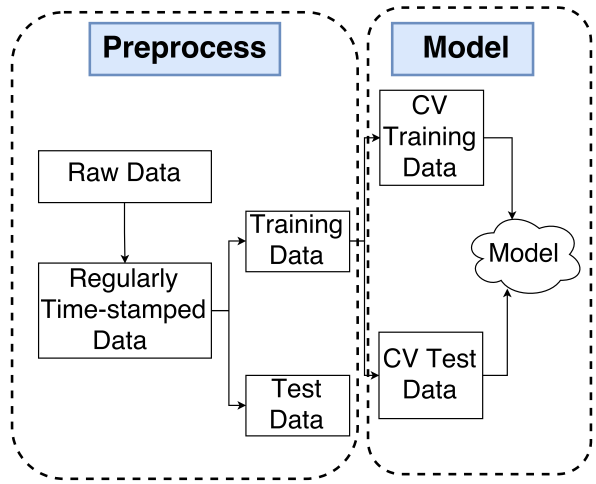

Figure 6. Overall flowchart.

response Y and a p-dimensional feature $\boldsymbol{x} = (x_1, \ldots, x_p)$, we have

$$\Pr(Y = i|x_1, \ldots, x_p) \propto \Pr(Y = i) \prod_{k=1}^{p} \Pr(x_k|Y = i)$$

based on Bayes' theorem and conditional independence assumption, and Naive Bayes classifies Y as

$$\hat{Y} = \operatorname{argmax}_i \Pr(Y = i|x_1, \ldots, x_p).$$

Despite its oversimplified and sometimes unrealistic conditional independence assumption, it often outperforms other more sophisticated algorithms. Naive Bayes is widely used in text mining and natural language processing.

Logistic regression (Hosmer Jr & Lemeshow, 2004) is widely used in classification problems. However, when the number of input features is large, it performs poorly due to overfitting. Penalized logisitic regression avoids the overfitting problems of logistic regression by imposing a penalty on large fluctuations in the estimated parameters. In this paper, we use a penalized logistic regression with ℓ_2 penalty. Besides avoiding overfitting and improving prediction accuracy, this ridge type penalty is also very computationally efficient.

Random forest (Breiman, 2001) is an ensemble learning method which averages over a large collection of de-correlated decision trees. Similar as bagging, random forest builds decision tress on bootstrapped samples. But unlike bagging method, when building the decision tree, each time random forest only use a portion of randomly selected features. Thus, it decorrelates the decision thees and makes their ensemble less variable. Random forest allows for interaction effects among features just like any tree based algorithm, but it corrects for the likely overfitting of decision trees. The performance of random forest is comparable to boosting, and they are easier to train and tune (J. Friedman, Hastie, & Tibshirani, 2001).

Gradient boosting machine (GBM) (J. H. Friedman, 2001, 2002) is an ensemble method which combines weak classifiers to form a strong classifier. We use decision tree as our weak classifier. Unlike random forest which fit a large number of decision trees in parallel, GBM works in a forward "stagewise" fashion. In each step, GBM firstly calculate the pseudo-residuals (negative first-order derivative of the loss function) at the current model, and then fit a decision tree to the pseudo-residuals. GBM then add the fitted decision tree to the previous model. There are many parameters that we can tune in GBM. For example, we can set the order of interaction we want to consider by specifying the depth of the decision tree; We can avoid overfitting by specifying a small learning rate in GBM. GBM is also very flexible as users can provide their own loss function. GBM has been implemented in many data mining competition winning strategies.

3.2. Evaluation

Evaluation is the key step to obtain feedback and find the approach that works well predicting faults with the data at hand. In this competition, each team was allowed to submit a set of predictions only once a week to score their model. However, this is not frequent enough given that there are a large number of possible models and tuning parameters to try. To remedy this problem and allow us to try many approaches, we built our own evaluation system, based on the idea of cross validation. Our cross validation system was basically designed to mimic the competition evaluation/scoring system.

To build our own scoring system, we randomly remove 50% of the faults in the second half of each training dataset. We build the model using the remaining fault data and attempt to

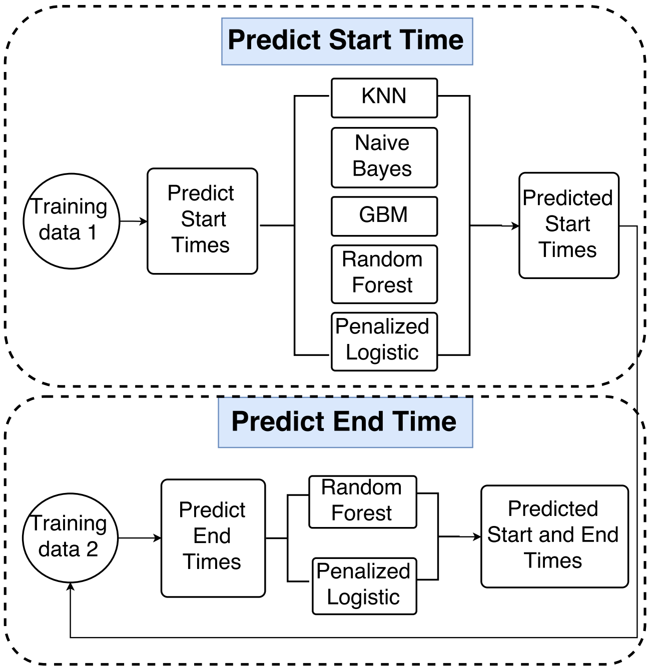

Figure 7. Modeling flowchart.

predict the deleted events. We then compare the predicted faults E_P with the deleted true events E_T, and score our model. If a fault event in E_T has been correctly predicted in E_P (i.e., there exists an event in E_P with start time and end time within one hour of actual start time and end time, and fault type also matches), it is a true positive and receives 10 point. If a fault event in E_P has correct start time and end time, and incorrect fault type, it is a misclassification and that prediction receives -0.01 point. If a fault event in E_P has incorrect start time or end time, it is considered as a false positive and receives -0.1 point. If a fault event in E_T has not been identified in E_P, it is considered a false negative and receives -0.1 point.

We found that the above scoring system worked very well in the sense that the order of magnitude of improvement of one classification algorithm over another based on our scoring system was similar to the improvement seen on the leader board. In this way, we could use our scoring system and experiment with many different algorithms and tuning parameters. The final model achieves a score of 79570 on the training data, and 21015 on the validation data. The average score per plant of the final model on the training data is 2411 with 90% confidence interval from 60 to 5006. The average score per plant on the validation data is 1401.

3.3. Feature engineering

We did feature engineering and added features like month, hour, weekday and time (the number of minutes since 00:00 of the first day of the corresponding year / (60*24)) in our classification models to predict faults' start and end time. A complete list of the features to predict faults' start and end time is given in Table 4. Here elapsed_t represents elapsed time since the fault first occurred which is defined in Section 3.5.

We also added lagged covariates of all sensor readings (R1-R4, S1-S4, E2 and E3) to the model. Specifically, for any sensor reading, $X(t)$, we included $X(t-k)$, for all nonzero k, where $k \geq$ min_lag and $k \leq$ max_lag. To define these new variables we introduce the following notation: $Lk\_mi\_Sj(t) = mi\_Sj(t-k)$, where $k > 0$ and thus, represents the lagged covariate of mi_Sj. In contrast, $Rk^*\_mi\_Sj(t) = mi\_Sj(t-k)$, where $k < 0$ and $k^* = -k$, and thus, represents the lead (future) covariate of mi_Sj. The time interval is 15 minutes. Based on the description of the competition, we know a fault is independent of data outside a three hour window of time. So the smallest min_lag and the largest max_lag we considered are -12 and 12, respectively. All covariates were standardized to have mean 0 and variance 1 before feeding to the classifiers.

3.4. Predict Start Time

For every plant and fault type in the cross validation training, test or validation datasets, we built a separate classification model to predict the start time of deleted events. $Start\_Fk$, the binary indicator of whether a type k fault starts within one hour, is the response variable Y. To train each model, we include all data from the first half of the sample where we know exactly when all faults do or do not occur. In addition, we also include data from the second half where $start\_Fk(t) = 1$. That is, we only include the data for the faults that we know occur (i.e., the faults that have not been randomly deleted). We define X_{train} and Y_{train} to be the resulting covariate and response matrices used to train the model. We stack the data from the second half that are not used to train the model to define X_{test}. X_{test} contains the data where the response $start\_Fk$ (Y_{test}) is unknown. We then estimate $\hat{p}_{\text{test}}$ ($p_{\text{test}} = \Pr(Y_{\text{test}} = 1)$), and predict deleted fault start time based on the magnitude of $\hat{p}_{\text{test}}$. We specify our model as follows to gain the optimal performance. The optimal tuning parameter and thresholds are found by cross validation.

- We tried different min_lag and max_lag combinations, and the best one we found is min_lag $= -8$ and max_lag $= 4$.
- For k consecutive estimates of p_{test} (i.e., the estimated probability a fault starts for k consecutive time intervals), we found the largest probability and compared it to a threshold p. If it exceeded p, the corresponding timestamp was saved as a predicted start time. We tested different combinations of values for k and p. The best performing combination was $k = 6$ and $p = 0.75$. See

model	**features in the model**
predict start time	month, hour, weekday, time, R1-R4, S1-S4, E2, E3 and lagged covariates of all sensor readings
predict end time	month, hour, weekday, time, R1-R4, S1-S4, E2, E3, elapsed_t and lagged covariates of all sensor readings

Table 4. Features include in the models.

Figure 8 for an illustration.

- We compared the performance of the various algorithms modeling covariates (month, hour, S3, R1, R2, R3, R4, etc) as categorical versus continuous variables. No real improvement was made modeling them as categorical variables, so all covariates are treated as continuous.
- We experimented with various different classifiers including KNN, Naive Bayes, GBM, random forest, and penalized logistic regression. We found that random forest and penalized logistic regression performed the best. Our final algorithm was an ensemble of these latter two models, where we kept all predicted start times from random forest, and then added all predicted start times that were found in penalized logistic regression but not found in random forest.

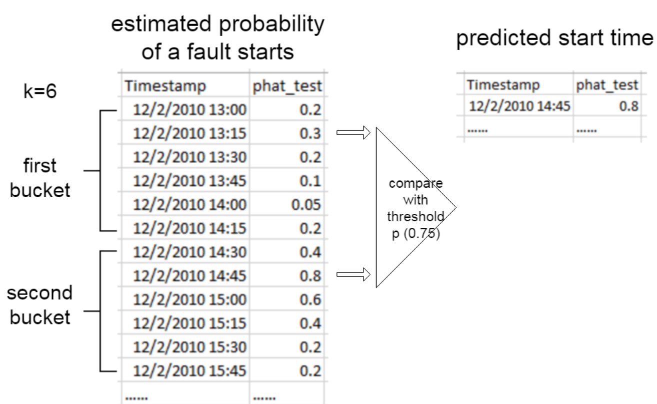

Figure 8. An example to predict the fault's start time.

One can determine which covariates are most important in predicting fault start times by looking at the random forest results. Each covariate can be scored based on mean decrease in impurity. Specifically, we add up the total amount that the Gini index is decreased by splits over a given predictor averaged over all trees, and this value is the measurement of feature importance. Gini index is defined as

$$G = \sum_{i=1}^{K} \hat{p}_{mk}(1 - \hat{p}_{mk}),$$

where $\hat{p}_{mk}$ represents the proportion of observations in the mth node that belongs to the kth class and K is the total number of classes (James, Witten, Hastie, & Tibshirani, 2013). Table 5 lists the top 15 most important covariates and their corresponding score (standardized) for each one of the five fault types in plant 1 and 6. The importance of covariates vary from fault to fault and from plant to plant. S3 is the most important covariate in predicting the start time of F1 in plant 1, while both R1 and S3 seem to be important in predicting F1's start time in plant 6; S3 is the most important covariate in predicting F2's start time, while E3 is the most important covariate in predicting F4's start time in plant 1.

Table 6 shows the percentage of times that each covariate ranked in the top 15 importance score (random forest to predict fault start time) averaged over all plants. S1-S4 seem to be more important than R1-R4, and the covariates time, month, E2 and E3 are also important features in the models.

3.5. Predict End Time

To predict the end time of a plant fault, we built another classification model. As with the start time prediction problem, we estimate a separate model for each fault type and plant. To explain our modeling approach, suppose we want to find the end time of a predicted type 1 fault ($F1$). We first estimate an upper bound for the duration of a $F1$ fault (t_{max}) based on all known $F1$ events. We estimate t_{max} as follows: $t_{\text{max}} = \max(8, q_{0.95})$, where $q_{0.95}$ is the 95% upper quantile of all historical F1 durations.

Intuitively, we could predict the fault end time by calculating the elapsed time since the fault first occurred. We denote it as elapsed_t which is measured in units of 15 minutes. We find that the model only based on elapsed_t isn't accurate enough, so we add other covariates to the model.

The classification model is trained using data from the t_{max} intervals following the onset of each known $F1$ event. These data, stacked together, form the matrix of covariates for the training model (X_{train}). end_F1, the binary indicator of whether fault 1 ends within one hour of the corresponding timestamp, serves as the response variable, Y_{train}. Once the classification model is trained, it is used to estimate the probability that each of our predicted events will end in any one of the t_{max} time periods following the predicted event start time. These predictions are based on X_{test}, formed by stacking the t_{max} intervals following the onset of each predicted $F1$ event.

Given the small penalty for false negative predictions relative to the reward for a true positive prediction, we allow our system to predict as many as two end times for each predicted event. The first estimated end time is made by finding the time period within the t_{max} periods following our predicted

Plant	Rank	F1		F2		F3		F4		F5	
		covariate	score	covariate	score	covariate	score	covariate	score	covariate	score
1	1	R4_m4_S3	0.0136	R1_m5_S3	0.0293	R7_m2_S4	0.0180	R5_n3_E3	0.0241	R4_m3_R1	0.0131
	2	R5_m4_S3	0.0118	R4_m5_S3	0.0268	R7_m2_S2	0.0179	n3_E3	0.0230	R8_m1_S1	0.0105
	3	R3_m4_S3	0.0104	R8_m5_S3	0.0247	R6_m2_S4	0.0163	R1_n3_E3	0.0194	R5_m5_S4	0.0099
	4	time	0.0095	R3_m5_S3	0.0245	R1_m5_S3	0.0153	R3_n3_E3	0.0179	R3_m3_R1	0.0091
	5	R8_m6_S3	0.0089	R2_m5_S3	0.0241	R2_m5_S3	0.0147	R6_n3_E3	0.0176	R7_m5_S2	0.0085
	6	R2_m4_S3	0.0088	R6_m5_S3	0.0229	R6_m5_S3	0.0146	R8_n3_E3	0.0166	R5_m3_R1	0.0084
	7	R7_m4_S3	0.0086	R7_m5_S3	0.0190	R6_m2_S2	0.0145	R2_n3_E3	0.0160	R7_m1_S1	0.0082
	8	L4_m6_S3	0.0073	R5_m5_S3	0.0181	R1_m2_S2	0.0143	R4_n3_E3	0.0139	R4_m5_S2	0.0081
	9	month	0.0072	L1_m5_S3	0.0169	R8_m2_S4	0.0140	R7_n3_E3	0.0137	R3_m1_S3	0.0080
	10	R5_m6_S3	0.0067	m5_S3	0.0119	R3_m5_S3	0.0137	R1_m2_S2	0.0131	m6_R1	0.0080
	11	R6_m4_S3	0.0067	L4_m5_S3	0.0108	m5_S3	0.0133	L1_m2_S2	0.0124	R1_m1_R1	0.0076
	12	R1_m4_S3	0.0060	R7_m2_S2	0.0095	R4_m5_S3	0.0130	L2_n3_E3	0.0116	R5_m1_S3	0.0076
	13	m4_S3	0.0059	R8_m2_S4	0.0088	R4_m2_S2	0.0125	R1_m2_S4	0.0114	L4_m2_S3	0.0073
	14	R4_m5_S3	0.0059	R7_m2_S4	0.0086	R8_m2_S2	0.0123	L1_n3_E3	0.0110	L1_m2_S3	0.0072
	15	R6_m6_S3	0.0058	R5_m2_S3	0.0080	R5_m2_S2	0.0119	L3_m2_S2	0.0104	R6_m2_S3	0.0070
6	1	R7_m1_S3	0.0110	L4_m7_S1	0.0116	L4_m7_S1	0.0151	R5_m8_S1	0.0187	R5_m8_S4	0.0244
	2	R3_m4_R1	0.0103	R3_m9_S3	0.0095	R4_m9_R2	0.0130	R6_m8_S1	0.0170	R4_n2_E3	0.0237
	3	R1_m4_R1	0.0095	R2_m9_S3	0.0090	R4_m9_S3	0.0122	R4_m8_S1	0.0155	R4_n1_E3	0.0197
	4	m4_R1	0.0095	R1_m9_S3	0.0084	L4_m3_S1	0.0119	R8_m8_S1	0.0151	R4_m8_S2	0.0195
	5	L2_m4_R1	0.0091	R4_m9_S3	0.0075	hour	0.0110	R7_m8_S1	0.0138	time	0.0160
	6	R7_m4_R1	0.0090	L3_m7_S1	0.0074	R8_m9_S1	0.0100	R2_m8_S1	0.0137	R1_m8_S2	0.0147
	7	R5_m4_R1	0.0079	R4_n1_E3	0.0070	R3_m9_S3	0.0092	R1_m8_S1	0.0124	R1_m8_S4	0.0147
	8	R8_m1_S3	0.0078	L1_m7_S1	0.0064	R4_m9_R3	0.0087	R3_m8_S1	0.0113	R5_m4_R1	0.0146
	9	R7_m7_S3	0.0072	R7_m7_S3	0.0064	R4_m9_R4	0.0084	m8_S1	0.0092	R7_m4_R1	0.0141
	10	R4_m7_S3	0.0070	m7_S1	0.0064	R5_m10_R2	0.0082	R5_n1_E3	0.0069	R3_m4_R3	0.0140
	11	time	0.0069	time	0.0062	R4_m9_S1	0.0082	R4_n1_E3	0.0064	R3_m4_R1	0.0132
	12	R2_m7_S3	0.0061	L4_m3_S1	0.0061	R6_m9_S1	0.0079	R2_n2_E3	0.0061	R5_n1_E3	0.0129
	13	R4_m4_R1	0.0061	L2_m7_S1	0.0059	R3_m9_S1	0.0078	R3_n2_E3	0.0059	R7_n2_E3	0.0128
	14	R7_n1_E2	0.0060	R5_m10_R2	0.0056	R5_m9_S1	0.0078	R2_n1_E3	0.0059	R4_m4_R3	0.0127
	15	R6_m7_S3	0.0059	R5_m9_S3	0.0053	R5_m10_R4	0.0076	R5_n2_E3	0.0057	R5_n2_E3	0.0126

Table 5. Top 15 most important covariates to predict fault start time for each of five faults in plant 1 and 6.

event with the largest estimated probability that end_F1=1. This is our first end time prediction. To look for a possible second prediction, we delete all observations with timestamps within one hour of our first estimated end time. We then find the (remaining) time period with the largest probability. If the estimated probability in this period is larger than our threshold $p2$, this is a second end time prediction. If the probability is less than $p2$, only one end time is predicted. See Figure 9 for an illustration, where the second end time prediction is $elapsed\_t = 7$ and is kept as $\hat{p} > p2(= 0.2)$.

The following list details the specifics of our final algorithm for the end time classification problem. The optimal tuning parameter and thresholds are found by cross validation.

- The optimal threshold probability for deciding on a second end time is $p2$=0.2.
- The optimal lag choice is min_lag $= -8$ and max_lag $=$ 8.
- We model all covariates as continuous variables.
- We have compared the performance of various different classifier methodologies including GBM, random forest, and penalized logistic regression. We find that GBM has the best performance. We choose tree_number=200 and tree_depth=5 for the GBM.

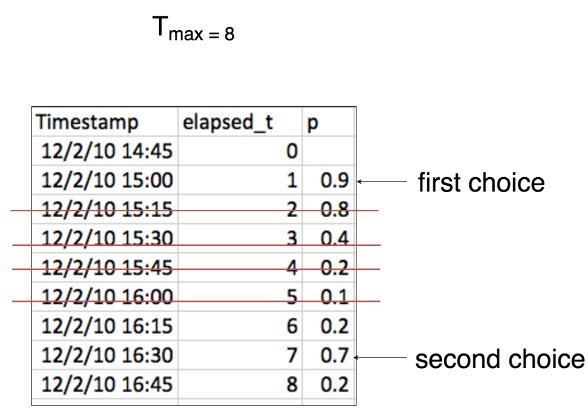

Figure 9. An example to predict the fault's end time.

As with the start times, we find the most important covariates in predicting fault end time by calculating a score based on mean decrease impurity in GBM. In Table 7 we list the top 15 most important covariates and their corresponding score in predicting fault end time for each one of the five fault types in plant 1 and 6. The most important covariate is elapsed_t, which ranks number one in all cases.

Table 8 shows the percentage of times that each covariate

Covariate	F1	F2	F3	F4	F5
time	60%	48%	31%	32%	18%
month	27%	14%	17%	11%	4%
hour	5%	12%	8%	4%	0%
weekday	2%	0%	0%	2%	2%
S1	32%	40%	81%	82%	64%
S2	54%	48%	58%	36%	88%
S3	65%	78%	33%	34%	20%
S4	49%	52%	56%	41%	90%
R1	19%	5%	10%	14%	10%
R2	17%	19%	23%	16%	14%
R3	19%	12%	8%	12%	12%
R4	2%	3%	6%	4%	4%
E2	19%	31%	12%	25%	8%
E3	25%	41%	17%	39%	16%

Table 6. Percentage that each covariate rank top 15 in the importance score (random forest to predict fault start time) averaged over all plants.

ranked in the top 15 importance score (GBM to predict fault end time) averaged over all plants. elapsed_t is the most important covariate. S1-S4 are again more important than R1-R4, and the covariates time, hour, weekday, E2 and E3 are also important features in the models.

4. CONCLUSION

In this paper, we proposed and implemented a machine learning based algorithm to detect industrial plant faults. The encouraging results demonstrated the usefulness of data-driven algorithms in fault detection of complex systems. Several extensions to our algorithms were considered but not implemented due to the time constraints of the PHM Society Data Challenge. These additional approaches are left as future work.

One such approach would be to not model each plant independently. Alternatively, we could try to first group the plants into clusters of like plants (based on like distributions and/or timing of faults, for example), and then model plants in each cluster together.

Another untried approach is deep learning neural networks. Convolutional neural networks or recurrent neural networks, which have been shown to be powerful tools when modeling with large and complex datasets, may yield good results. Convolutional neural network can automatically consider lagged observations by modeling temporal contiguous observations jointly together. Recurrent neural network can create an internal state of the network which allows it to exhibit dynamic temporal behavior. These facts make deep learning neural networks potentially very useful in fault detection for the PHM data.

Lastly, in our approach, lagged covariates are added to the model which creates high dimensional features. Curse of dimensionality may damnify the classifiers' performances. Techniques such as principal component analysis and functional data analysis can be applied to extract key features from time series covariates and reduce the feature dimension.

ACKNOWLEDGMENT

The author wants to give thanks to SAS colleges Anya Mcguirk, Sergiy Peredriy, Arin Chaudhuri, Alex Chien, Deovrat Kakde and Gul Ege for their help in the Prognostics and Health Management Society 2015 data challenge competition.

REFERENCES

Aldrich, C., & Auret, L. (2013). *Unsupervised process monitoring and fault diagnosis with machine learning methods*. Springer.

Breiman, L. (2001). Random forests. *Machine learning*, *45*(1), 5–32.

Chiang, L. H., Kotanchek, M. E., & Kordon, A. K. (2004). Fault diagnosis based on fisher discriminant analysis and support vector machines. *Computers & chemical engineering*, *28*(8), 1389–1401.

Chiang, L. H., Russell, E. L., & Braatz, R. D. (2000). Fault diagnosis in chemical processes using fisher discriminant analysis, discriminant partial least squares, and principal component analysis. *Chemometrics and intelligent laboratory systems*, *50*(2), 243–252.

Friedman, J., Hastie, T., & Tibshirani, R. (2001). *The elements of statistical learning* (Vol. 1). Springer series in statistics Springer, Berlin.

Friedman, J. H. (2001). Greedy function approximation: a gradient boosting machine. *Annals of statistics*, 1189–1232.

Friedman, J. H. (2002). Stochastic gradient boosting. *Computational Statistics & Data Analysis*, *38*(4), 367–378.

He, Q. P., & Wang, J. (2007). Fault detection using the k-nearest neighbor rule for semiconductor manufacturing processes. *Semiconductor manufacturing, IEEE trans-*

Plant	Rank	F1		F2		F3		F4		F5	
		covariate	score	covariate	score	covariate	score	covariate	score	covariate	score
1	1	elapsed_t	0.0707	elapsed_t	0.1406	elapsed_t	0.2616	elapsed_t	0.2444	elapsed_t	0.1472
	2	time	0.0285	time	0.0338	time	0.0374	L1_m3_S1	0.0186	L1_m3_S1	0.0678
	3	L1_m4_S3	0.0182	L1_m5_S1	0.0121	L1_m5_S1	0.0101	L2_m3_S1	0.0131	time	0.0574
	4	R8_m4_S3	0.0155	R8_m2_S3	0.0116	hour	0.0098	L3_m6_S1	0.0127	L2_m3_S1	0.0516
	5	R7_m4_S3	0.0110	R8_m2_S1	0.0110	L1_m2_S1	0.0092	L2_m6_R1	0.0104	L3_m2_S1	0.0159
	6	L2_m4_S3	0.0093	L1_m2_S1	0.0095	L8_m2_S1	0.0076	R6_n3_E2	0.0088	L3_m3_S1	0.0142
	7	R8_m1_S4	0.0076	R7_m2_S1	0.0091	R3_n2_E2	0.0074	R4_m3_S1	0.0085	L6_m5_S1	0.0093
	8	L1_m4_S4	0.0070	hour	0.0083	weekday	0.0065	time	0.0083	L1_m3_S2	0.0088
	9	R8_m1_S3	0.0069	R6_m2_S1	0.0079	R8_m4_S4	0.0059	R2_m3_S1	0.0075	R8_m1_S1	0.0087
	10	R5_m4_S3	0.0067	L1_m3_S1	0.0075	R8_m2_S4	0.0056	R6_n3_E3	0.0075	R8_m3_S1	0.0075
	11	R6_m4_S4	0.0066	L2_m5_S1	0.0073	L2_m5_S1	0.0055	R5_m2_S1	0.0074	R8_m1_S4	0.0074
	12	R7_m1_S4	0.0064	R8_m5_S1	0.0067	L2_m2_S1	0.0051	weekday	0.0073	L1_m2_S1	0.0068
	13	R8_m4_S4	0.0063	R8_m5_S4	0.0063	L5_m2_S1	0.0048	L1_m6_R1	0.0068	L8_m6_S1	0.0066
	14	L2_m1_S4	0.0062	L1_m2_S4	0.0060	L8_m1_S1	0.0048	R8_n3_E3	0.0066	L5_m4_S1	0.0064
	15	L2_m4_S4	0.0061	R8_m5_S2	0.0060	R7_n3_E2	0.0046	R3_n3_E2	0.0063	L1_m3_S4	0.0064
6	1	elapsed_t	0.1210	elapsed_t	0.1633	elapsed_t	0.0934	elapsed_t	0.3109	elapsed_t	0.1330
	2	time	0.0292	time	0.0434	L1_m9_S1	0.0683	L2_m8_S1	0.0380	time	0.0276
	3	R8_m9_S3	0.0111	R8_m9_S3	0.0144	R8_m9_S1	0.0365	L1_m8_S1	0.0366	R8_m8_S4	0.0151
	4	L1_m9_S3	0.0100	L1_m9_S3	0.0114	m6_S1	0.0229	L8_m3_S4	0.0263	L1_m8_S2	0.0147
	5	R8_m10_S3	0.0081	L1_m9_S1	0.0067	L1_m6_S1	0.0224	L8_m3_S2	0.0167	R8_m8_S2	0.0144
	6	hour	0.0071	L1_m9_S2	0.0060	L1_m3_S1	0.0162	L1_m3_S4	0.0166	L1_m8_S4	0.0118
	7	L1_m10_S3	0.0059	R7_m9_S3	0.0059	L1_m4_R1	0.0161	L1_m6_S1	0.0164	R8_m8_S1	0.0113
	8	L1_m10_S4	0.0058	L1_m9_S4	0.0055	L6_m9_S4	0.0115	L1_m3_S2	0.0151	R6_m8_S1	0.0081
	9	L1_m7_S2	0.0052	R8_m1_S3	0.0053	n1_E2	0.0095	m7_S1	0.0124	L1_m8_S1	0.0073
	10	R8_m9_S4	0.0051	L2_m9_S3	0.0048	m8_S1	0.0086	R8_m8_S1	0.0117	L2_m8_S1	0.0072
	11	L1_m7_S4	0.0046	R8_n2_E2	0.0047	L6_m9_S2	0.0082	L1_m7_S1	0.0109	L8_m8_S1	0.0072
	12	weekday	0.0045	R8_m9_S1	0.0047	L2_m9_S1	0.0076	R8_n1_E3	0.0092	R4_m8_S1	0.0070
	13	R7_m10_S1	0.0044	L1_m1_S3	0.0044	L1_m2_S1	0.0075	m3_S2	0.0089	L7_m2_S1	0.0069
	14	R8_n1_E3	0.0043	hour	0.0042	R5_m9_S4	0.0059	L1_m10_S1	0.0085	R8_m1_S1	0.0067
	15	R8_m9_S1	0.0042	L1_m7_S3	0.0042	R7_m4_S4	0.0057	R4_m6_S1	0.0081	R5_m8_S1	0.0062

Table 7. Top 15 most important covariates to predict fault end time for each of five faults in plant 1 and 6.

actions on, *20*(4), 345–354.

Hosmer Jr, D. W., & Lemeshow, S. (2004). *Applied logistic regression*. John Wiley & Sons.

James, G., Witten, D., Hastie, T., & Tibshirani, R. (2013). *An introduction to statistical learning* (Vol. 112). Springer.

Korbicz, J., Koscielny, J. M., Kowalczuk, Z., & Cholewa, W. (2012). *Fault diagnosis: models, artificial intelligence, applications*. Springer Science & Business Media.

Lee, S., Park, W., & Jung, S. (2014). Fault detection of aircraft system with random forest algorithm and similarity measure. *The Scientific World Journal*, *2014*.

Rish, I. (2001). An empirical study of the naive bayes classifier. In *Ijcai 2001 workshop on empirical methods in artificial intelligence* (Vol. 3, pp. 41–46).

Rosca, J., Song, Z., Willard, N., & Eklund, N. (2015). *PHM15 Challenge Competition and Data Set: Fault Prognostics, NASA Ames Prognostics Data Repository (http://ti.arc.nasa.gov/project/prognostic-data-repository), NASA Ames Research Center, Moffett Field, CA*.

Samanta, B. (2004). Gear fault detection using artificial neural networks and support vector machines with genetic algorithms. *Mechanical Systems and Signal Processing*, *18*(3), 625–644.

Wang, L., & Yu, J. (2005). Fault feature selection based on modified binary pso with mutation and its application in chemical process fault diagnosis. In *Advances in natural computation* (pp. 832–840). Springer.

Yin, S., Ding, S. X., Haghani, A., Hao, H., & Zhang, P. (2012). A comparison study of basic data-driven fault diagnosis and process monitoring methods on the benchmark tennessee eastman process. *Journal of Process Control*, *22*(9), 1567–1581.

Covariate	**F1**	**F2**	**F3**	**F4**	**F5**
elapsed_t	98%	95%	93%	93%	95%
time	94%	89%	78%	79%	63%
month	0%	0%	0%	0%	0%
hour	57%	58%	50%	45%	12%
weekday	21%	25%	35%	30%	12%
S1	65%	86%	98%	100%	100%
S2	90%	91%	91%	73%	98%
S3	89%	82%	20%	12%	14%
S4	97%	93%	93%	73%	95%
R1	11%	18%	15%	25%	9%
R2	2%	2%	4%	7%	5%
R3	2%	7%	11%	9%	7%
R4	0%	2%	7%	7%	7%
E2	22%	33%	35%	30%	16%
E3	29%	37%	37%	32%	40%

Table 8. Percentage that each covariate rank top 15 in the importance score (GBM to predict fault end time) averaged over all plants.